Differential Reactions of Microglia to Brain Metastasis of Lung Cancer

Bei Ping He,[1] Jian Jun Wang,[2] Xian Zhang,[1] Yan Wu,[1] Miao Wang,[3] Boon-Huat Bay,[1] and Alex Yuang-Chi Chang[3,4]

[1]Department of Anatomy, Yong Loo Lin School of Medicine, National University of Singapore, Singapore; [2]Department of Pathology, Changhai Hospital, Shanghai, China; [3]Division of Johns Hopkins in Singapore; [4]Johns Hopkins Singapore International Medical Centre, Singapore

The brain is a common metastatic site for various types of cancers, especially lung cancer. Patients with brain metastases have a poor prognosis in spite of radiotherapy and/or chemotherapy. It is postulated that immune cells in the brain may play a major role in cancer metastasis, dormancy, and relapse. Although microglia may serve as a major component in the brain immune system, the interaction between metastatic cancer cells and microglia is still largely unknown and remains to be elucidated. In this study, we have investigated microglial reactions in brain tissues with metastatic lung cancer cells and evaluated the cytotoxic effects of lipopolysaccharide (LPS)-activated microglia on metastatic lung cancer cells in vitro. In the vicinity of metastatic lung cancer mass in the brain, microglia showed signs of significant activation. There was an obvious increase in the number of microglia labeled with ionized calcium binding adaptor molecule 1 (Iba-1) antibody, a specific marker of microglia. The microglia were observed to form a clear boundary between the tumor mass and normal brain tissue. In the region where the tumor mass was situated, only a few microglia expressed inducible nitric oxide synthase (iNOS) and tumor necrosis factor-α (TNF-α), indicating differential activation in those microglia. The supernatant from LPS-activated microglia induced apoptosis of metastatic lung cancer cells in vitro in a dose- and time-dependent manner. However, at lower concentrations of activated microglial supernatant, trophic effects on cancer cells were observed, some lung cancer cells being insensitive to microglial cytotoxicity. Together with the observation that TNF-α alone induced proliferation of the tumor cells, the findings provide possible clues to the mechanism involved in metastasis of lung cancer cells to the brain.

Online address: http://www.molmed.org
doi: 10.2119/2006–00033.He

INTRODUCTION

The brain is an important organ in the metastasis of lung cancer cells (1-3) and one of the major sites of distant relapse in patients with lung cancer and other cancers (4). Obviously, the prevention of brain metastasis is of importance in cancer management (4).

The successful homing in and growth of metastatic lung cancer cells in the brain parenchyma appears to suggest failure of the immune defense in the brain environment. Owing to the existence of the blood–brain barrier (BBB), the immunological mechanism in the central nervous system (CNS) is believed to be different from that in peripheral tissues. The unique structure of the BBB, which is formed by endothelial cells, basal lamina, and astrocytes, isolates central cells from peripheral tissues and maintains highly stable conditions within the CNS. The impermeability of the BBB could prevent entrance of immunoglobulins and invasion of leukocytes from the blood (5) and limit the delivery of most cytotoxic agents into the brain (6,7), thereby resulting in ineffective chemotherapy in the treatment of brain metastases and hindrance of immune reactions against metastatic lung cancer cells. The BBB has failed to block the invasion of metastatic lung cancer cells into brain parenchyma in many patients, however, suggesting the presence of some mechanisms that facilitate invasion of cancer cells into the brain parenchyma through the BBB. It is likely that cell–cell interactions play a crucial role in this mechanism; however, interactions between tumor cells and various types of cells inside the brain are not fully understood.

Microglia are believed to be the most important immune cells in the CNS, as most other inflammatory cells are largely excluded from the CNS. Microglia constitute the tissue macrophages of the CNS and express many features of monocytes, including activation of signaling cascades well described in the immune system (involving chemokines and cytokines and their receptor systems). Under physiological conditions, resident microglia are quiescent and scattered ubiquitously throughout the CNS. Upon activation, they begin to proliferate, migrate toward the impaired region, change morphology from their ramified resting status into hypertrophic and finally ameboid activated forms, and become phagocytotic. Microglia are thought to play a critical role in host defense against microorganisms and malignant cells and in the pathological processes of neurodegeneration (8).

Address correspondence and reprint requests to *Bei Ping He, Department of Anatomy, Yong Loo Lin School of Medicine, National University of Singapore, 4 Medical Drive, Singapore 117597. Phone: (65) 6516 7809; fax: (65) 6778 7643*
Submitted April 21, 2006; accepted for publication July 22, 2006.

It has been discovered, however, that inflammatory cells such as peripheral macrophages, the siblings of microglia, are double-edged swords in cancer progression. Primarily, they play a role in destroying the malicious cells; on the other hand, they are able to secrete factors necessary for cancer development (9). The evidence suggests that stromal cells in vicinity of the peripheral cancer cells—including fibroblasts, inflammatory cells such as macrophages, neutrophils, and lymphocytes—could interact with cancer cells. Upon activation, the tumor-associated macrophages could release a vast diversity of growth factors, proteolytic enzymes, cytokines, and inflammatory mediators that may facilitate cancer metastasis. Interestingly, significant microglial activation has been detected in the vicinity of glioma tumor cells (10,11). There is also evidence that microglia/macrophages attracted by gliomas could actually promote tumor growth (12,13). Monocyte chemoattractant protein 1 (MCP-1) released from MCP-1–transfected glioma cells induced a significant chemotactic activity for microglial cells in vitro and in vivo, and the recruited microglial cells have further been found to promote tumor growth in vivo (14). In addition, to suppress the antigen-presenting ability of microglial cells (15), some cytokines, such as IL-10 released from activated microglia (16), could be involved in local immunosuppression and progression of glioma, especially enhancing proliferation of tumor cells and their infiltration into surrounding normal brain tissue (13,17). In their analysis of the expression of 53 cytokines and their receptors in samples of glioblastoma and human malignant glioma cell lines, Hao et al. (18) reported that tumor cells expressed more cytokines related with immunosuppression, which could therefore result in the failure of immune defense against tumor cells.

However, the facilitating role of microglia in metastasis has been surprisingly accompanied by a lower indicence of glioma tumor cells migrating out of the brain parenchyma (19). The findings of the metastasis-facilitating role of peripheral macrophages and restricted distant metastasis of glioma have suggested that there are possibly differences between peripheral macrophages and central microglia in their responses to tumor cells and that differences may also exist in microglial reactions toward primary brain tumor cells in comparison to that toward cancer cells that have metastasized to the brain. Therefore, it would be of interest to investigate the functional aspects of microglia in invasion, dormancy, and relapse of brain metastatic cancers. In the current study, immunohistochemistry has been employed to identify the activation of microglia toward metastatic lung cancer cells in the excised brain tissues from surgical operations, and cytotoxicity assays have been carried out to evaluate the effects of microglial factors on metastatic lung cancer cells in vitro.

MATERIALS AND METHODS

Patients

We used archival brain tumor tissues with metastasis of lung cancer cells from 8 lung cancer patients who underwent neurological surgery. All cases were clinically and pathologically classified as stage IV lung adenocarcinoma. Metastases were found in the frontal lobe (n = 4) and temporal lobe (n = 3), and 1 patient had metastatic tumors in the frontal, temporal, and parietal lobes. Six-micrometer sections of the formalin-fixed and paraffin-embedded brain tissues were used for immunohistochemical study.

Immunohistochemistry

To determine activation of microglia in these patients, the ionized calcium binding adaptor molecule-1 (Iba-1) has been selected as a specific marker for microglia (20), and the expression of inducible nitric oxide synthase (iNOS) and tumor necrosis factor-α (TNF-α) as a functional assessment for microglial activation. The slides were deparaffinized and rehydrated following standard protocol before immersion in 0.25% trypsin in PBS at 37 °C for 15 min for antigen retrieval, followed by incubation with 3% H_2O_2 in PBS (pH 7.4) for 5 min at room temperature to eradicate endogenous peroxidase in the human brain. After incubation with 1.5% normal serum, antibodies of Iba-1 (1:2000; Wako, Japan), iNOS (1:1000; Santa Cruz Biotechnology, UK), TNF-α (1:200; Chemicon International, USA), glial fibril acidic protein (GFAP), a marker for astrocytes (1:1500; DakoCytomation, Denmark), and neurofilament heavy subunit (NFH), a marker for neurons (1:5000; Chemicon International) were applied to sections on the slides overnight at room temperature. The sections were incubated with biotinylated anti-rabbit IgG (1:200; Vector Laboratories, USA) for 1 h at room temperature, and then the secondary antibodies were localized with *Elite* ABC with 0.05% 3-3′ diaminobenzidine tetrachloride (DAB) (Sigma, USA) as the peroxidase substrate. The sections were finally counterstained with methyl green and coverslipped with permount after dehydration and clearance.

For microglial double labeling, sections were first incubated with rabbit anti-iNOS (1:200) or TNF-α (1:200) for 2 h, followed by incubation of goat-anti-rabbit IgG conjugated with Cy3 (1:200, red) and lectin conjugated with FITC (1:200, green) at room temperature for 1 h. For astrocytic double labeling, a mixture of mouse-anti-GFAP (1:200) and rabbit anti-iNOS (1:200) or TNF-α (1:200) was applied to the sections for 2 h before incubating them with a mixture of goat anti-mouse IgG conjugated with FITC (1:200) and goat anti-rabbit IgG conjugated with Cy3 (1:200) for 1 h at room temperature. The sections were covered by coverslips using the mount medium with DAPI (which stains nuclei bluish purple).

Cells and Cell Culture

Lung cancer cells overlaid with supernatant from a microglial cell line were employed to study effects of activated microglia on lung cancer cells. Lung cancer cells were harvested and cloned from pleural effusion of a patient who suffered from extensive non–small cell lung cancer.

The cells were cultured in RPMI 1640 (Sigma) supplemented with 10% heat-inactivated fetal bovine serum (FBS) (Hyclone, Germany), 1% antibiotics, 1% L-glutamine, and 1% of 10 mM Hepes buffer. Murine immortalized microglial BV-2 cells (21,22) were routinely maintained at 37 °C and 5% CO_2 in DMEM (Sigma) supplemented with 10% heat-inactivated FBS. Cells were grown in 75-cm^2 plastic flasks and split twice a week at different cell densities using 10 mM EDTA according to standard procedures.

Activation of Microglia

The BV-2 cells were allowed to grow to confluence and then exposed to 1 μg/mL lipopolysaccharide (LPS) (Sigma) in 10 mL serum-free DMEM for 24 h. The supernatant, referred to as LPS-activated BV-2 conditioned medium (LPS-BVCM), was collected, centrifuged, filtered through a 0.22-μm filter, and stored at –80 °C before use. The supernatant from BV-2 cells without LPS stimulation and normal serum-free DMEM served as controls.

The method of assaying toxicity of LPS-BVCM over neuronal cells has been described (22). To confirm the activation of the BV-2 microglial cells in the current study, the release of TNF-α by LPS-activated microglia was further measured using the DuoSet mouse TNF-α ELISA kit (R&D Systems, USA) following the manufacturer's instructions. Briefly, 96-well ELISA plates were coated with goat anti-mouse TNF-α capture antibody and incubated overnight at 4 °C. The plates were washed 3 times with PBS containing 0.05% Tween 20 and blocked by PBS with 1% bovine serum albumin (BSA) and 5% sucrose. After the addition of samples and serial dilutions of standard antigen, plates were incubated for 2 h at room temperature. Biotinylated goat anti-mouse TNF-α antibodies were used as the detection antibody, and streptavidin-horseradish peroxidase was added to each well as the conjugate. Equal proportions of hydrogen peroxide and tetramethylbenzidine were used as the substrate solution, and sulfuric acid was used to stop the reaction. All samples and standards were run in triplicate, and optical density was determined with a microplate reader at 450 nm.

The iNOS expression and NO production were also used to verify the activation of the microglia 24 h after the application of LPS. The iNOS protein expression was observed using Western blot. Briefly, the BV-2 cells were homogenized with lysis buffer. The protein preparation (25 μg) was separated using 10% SDS-polyacrylamide gels and electrotransferred to a polyvinylidene difluoride (PVDF) membrane. Nonspecific binding sites on the PVDF membrane were blocked by incubation with 5% nonfat milk in 0.1% Tween-20 TBS (TTBS) for 1 h. The PVDF membrane was then incubated overnight in monoclonal antibody to iNOS (1:200) in 1% BSA in TTBS followed by incubation of horseradish peroxidase–conjugated goat anti-mouse IgG (1:5000; Pierce, USA) for 1 h at room temperature. Immunoreactivity was visualized using a chemiluminescent substrate (Supersignal West Pico; Pierce). Loading controls were carried out by incubating the blots at 50 °C for 30 min with stripping buffer (100 mM 2-mercaptoethanol, 2% SDS, and 62.5 mM Tris–hydrochloride, pH 6.7), followed by reprobing using a mouse monoclonal antibody against β-actin (1:5000; Sigma) and horseradish peroxidase–conjugated anti-mouse IgG (1:5000; Pierce). Exposed films containing blots were scanned, but the measurement for the band density was omitted, as there was no iNOS expression in BV-2 cells without LPS stimulation. Intracellular NO generation was monitored by coculturing the BV-2 cells on the coverslips in the 6-well plate with 10 μM 4,5-diaminofluorescein diacetate (DAF-2DA) (Calbiochem, USA) (23). Twenty-four hours after LPS stimulation, the DAF-2DA was added to the wells for 2 h, and the cells were fixed using 4% paraformaldehyde in PBS for 10 min at 4 °C. The coverslips were mounted on slides and viewed under a fluorescence microscope.

Cell Treatment and MTT Assay

Cell viability served as an assessment method to evaluate effects of activated microglia on the lung cancer cells. MTT [3-(4,5-dimethylthiazole-2yl)-2,5-diphenyltetrazolium bromide] (Sigma) was dissolved at a concentration of 1 mg/mL in sterile PBS at room temperature, and the solution was further sterilized by filtration and stored at 4 °C in the dark.

One milliliter per well of suspension containing the metastatic lung cancer cells was plated in 24-well plates at the density of 5×10^5 cells/mL. Two days later, the cells were treated with 10%, 25%, 50%, 75%, or 100% LPS-BVCM in serum-free RPMI 1640 for 12, 24, 36, or 48 h. The cellular effect of TNF-α alone on the lung cancer cells was also evaluated by MTT assay. Recombinant mouse TNF-α (Chemicon, USA) at 0.388, 0.97, 1.94, 2.91, and 3.88 ng/mL was added into the same amount (5×10^5 cells/well) of the cancer cells seeded in 24-well plates. The concentrations of recombinant TNF-α corresponded to TNF-α concentrations in 10%, 25%, 50%, 75%, and 100% LPS-BVCM based on the TNF-α ELISA results. Then 1 mL of 1 mg/mL MTT solution was added to each well for 2-h incubation at 37 °C. The precipitate in each well was resuspended in 1 mL DMSO (Sigma). After 1 h further incubation, absorbance was measured at 570 and 630 nm using a spectrophotometric microplate reader (Multiskan EX, Labsystems, Finland). Cell viability was calculated by the following formula:

$$\text{Cell viability (\%)} = \frac{\text{OD570 (Test} - \text{Blank)} - \text{OD630 (Test} - \text{Blank)}}{\text{OD570 (Control} - \text{Blank)} - \text{OD630 (Control} - \text{Blank)}} \times 100$$

Annexin V Staining

Phosphatidylserine (PS) is asymmetrically located in the lipid bilayer of the plasma membrane in mammalian cells. In cells undergoing apoptosis, PS is transferred from the cytoplasmic surface of the cell membrane to the outer surface

of the plasma membrane and therefore serves as an early marker for apoptosis. The level of apoptosis was assessed using BD ApoAlert Annexin V kit (FITC conjugate; BD Biosciences, USA) after the cancer cells were treated with various concentrations of LPS-BVCM according to manufacturer's instructions. Briefly, tumor cells were seeded onto collagen-coated coverslips in 6-well plates and then treated with the above concentrations of LPS-BVCM for 12, 24, 36, and 48 h. At each time interval, the cells were rinsed with 1× binding buffer, followed by the addition of 5 μL annexin stain and 10 μL propidium iodide (PI) and incubated for 15 min at room temperature in the dark. The cells were then fixed using 4% paraformaldehyde and detected by an Olympus Fluoview 1000 confocal microscope; 10 photos were randomly taken from each slide for cell counting. Viewed under a confocal or fluorescence microscope, the normal cells will not be labeled with any fluorescence, but apoptotic cells will be labeled with green fluorescence. The fluorescent dye PI, which stains nucleic acids red, will be excluded from viable and apoptotic cells with integral cell membranes. The PI-positive staining indicates apoptotic cells at late stage or necrotic cells.

Data Analysis

All the experiments were repeated at least in triplicate for statistical purposes, and where appropriate the data are presented as mean ± SD. Statistical analyses were performed by 1-way ANOVA for independent variables. The level of significance was set at $P < 0.05$.

RESULTS

Immunohistochemistry

The mass of metastatic cancer cells in the brain could be clearly identified as a NFH-negative region because neurons and their processes positively stained with anti-NFH antibody were evenly distributed in the normal brain parenchyma; however, no positive staining could be observed within the region

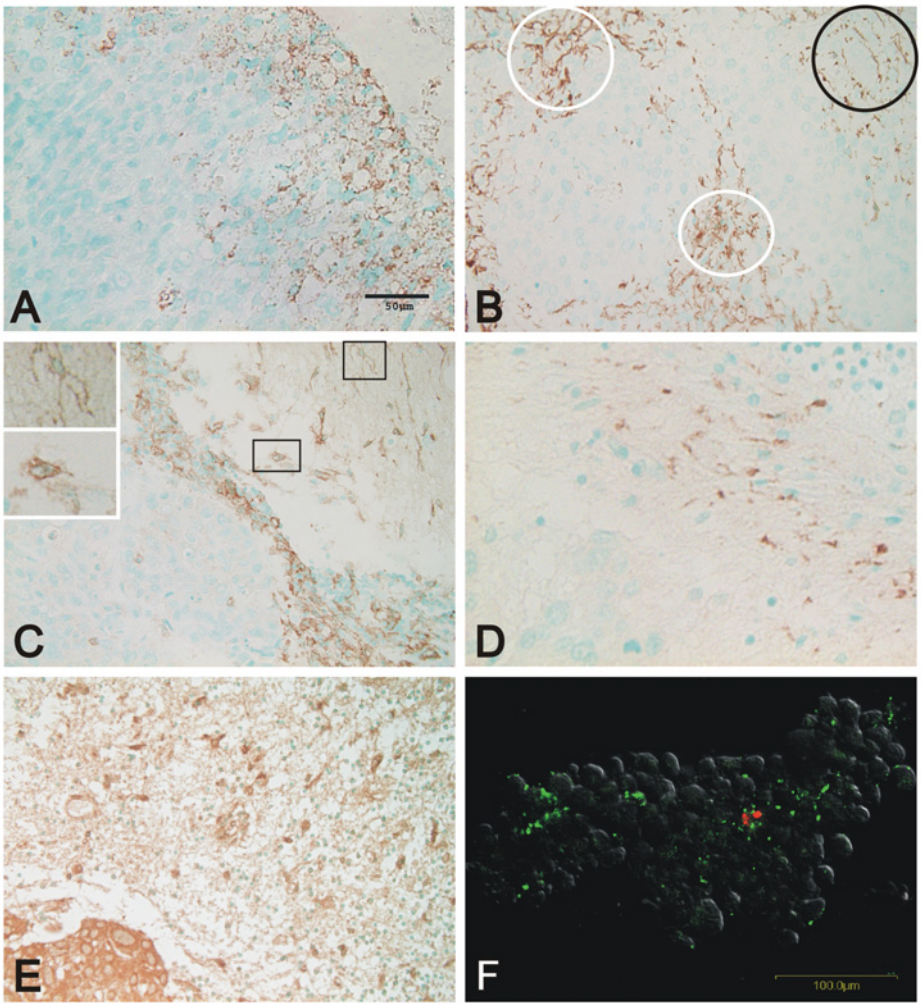

Figure 1. Immunohistochemical staining of paraffin-embedded brain section with metastatic lung cancer. (A) Neurons positively stained with anti-NFH antibody were evenly distributed in the brain tissue; however, no positive staining could be observed in the region where there is aggregation of the cancer cells. Note that no clear boundary can be observed between neurons and tumor cells in this staining. (B) GFAP-positive astrocytes surround tumor masses, which show as clear regions in the micrograph. Hypertrophy of GFAP-positive cells can be observed in the vicinity of cancer masses (in white circle) compared with normal astrocytes (in black circle). Note that the boundary between cancer cells and astrocytes is slightly diffused. (C) A dense layer of Iba-1–positive microglia has accumulated to form a clear wall surrounding the tumor mass and shows negative staining to Iba-1 antibody (at the right lower-view field). In the area close to the cancer cells, microglia show as round cells (lower inset), whereas microglia with longer processes (upper inset) can be noted in the area away from the cancer cells. (D) Within the tumor mass, TNF-α–positive cells are barely observed. A number of positive cells are present in the surrounding area, although no sharp boundary can be noted between TNF-α–positive cells and tumor mass. (E) Strong iNOS staining is observed within the whole region of tumor mass. In the vicinity of the tumor mass, iNOS-positive cells are scattered in the brain tissue. Note the absence of a wall of iNOS-positive cells surrounding the tumor mass. (F) Annexin V staining of metastatic lung cancer cells treated with LPS-BVCM in vitro. The photo was taken 24 h after the cancer cells were treated with 50% LPS-BVCM in the culture medium. The green color indicates the apoptotic cells and red the necrotic cells. Scale bars are 50 μm in A–E and 100 μm in F.

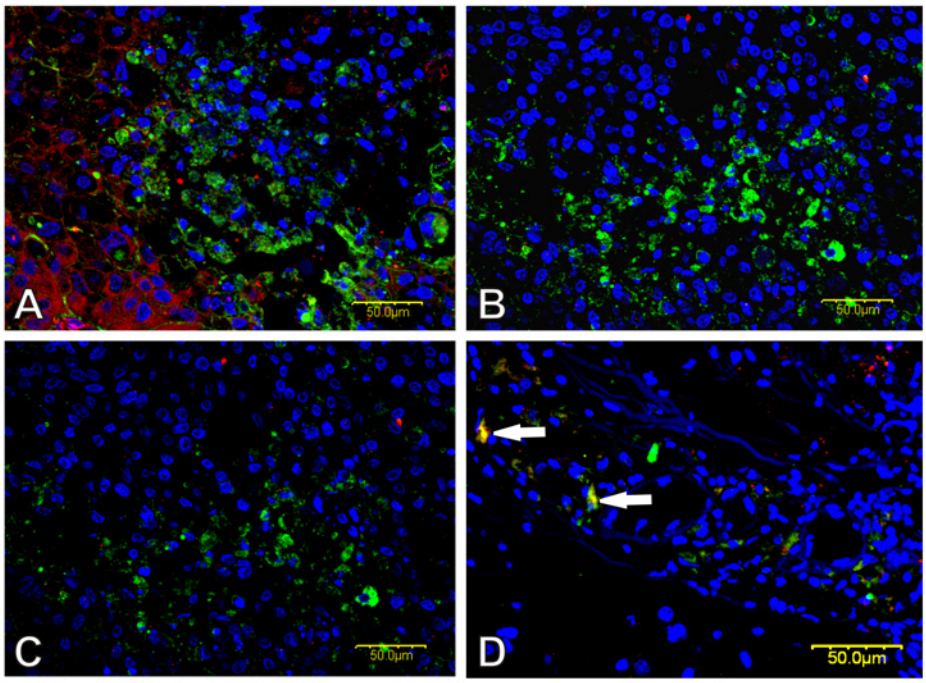

Figure 2. Double immunolabeling for (A) lectin (for microglia and endothelium, green) and iNOS (red); (B) lectin (green) and TNF-α (red); (C) GFAP (for astrocytes, green) and iNOS (red); and (D) GFAP (green) and TNF-α (red). The DAPI (purple) stains the nuclei in all micrographs. A dense population of lectin-positive cells (microglia or endothelia, green) is observed in A and B. However, most lectin-positive cells are not colocalized with either iNOS (A) or TNF-α (B). The GFAP-positive cells (green) are not labeled with iNOS (C), but a few GFAP-positive astrocytes express TNF-α (D, yellow cells indicated by arrows). Some GFAP-negative cells are found to express TNF-α at the left upper-view field of D. Bar = 50 μm.

with cancer cell aggregation (Figure 1A). Numerous astrocytes with hypertrophic morphology could be observed in the vicinity of metastatic lung cancer masses. The aggregation of cancer cells has been observed as a clear region among the GFAP-positive astrocytes (Figure 1B). A conspicuous boundary was observed between the cancer cell mass and Iba-1–positive microglia in the brain tissue (Figure 1C). The Iba-1–positive microglia were tightly packed to form a dense microglial "wall," in contrast to the scattered microglial distribution in the region situated away from the wall. In addition, microglia in or close to the wall showed round ameboid morphology, whereas branching ramified microglia could be observed in the brain region slightly away from the cancer mass, indicating microglial transformation from ramified resting to ameboid activated microglia. A few TNF-α–positive cells were noted in the region close to the cancer masses (Figure 1D), but the TNF-α–positive cells failed to form a wall like that of the Iba-1–positive cells. No TNF-α–positive cells were found within the cancer mass. In the vicinity of the cancer cell mass, only a few iNOS-positive cells were scattered in the brain parenchyma (Figure 1E), indicating that most activated microglia were not induced to increase production of nitric oxide (NO). In metastatic tumor parenchyma, no astrocytes wer found, and occasionally very few Iba-1–positive cells were noted. We have not determined if these Iba-1–positive cells were infiltrated macrophages or macrophages in blood vessels. No TNF-α–positive cells were detected. Interestingly, cancer cells showed strong positive staining to the iNOS antibody.

In the double labeling, most lectin-positive activated microglia (green) were not colocalized with either iNOS (Figure 2A) or TNF-α (Figure 2B) when viewed under a confocal microscope. The GFAP-positive cells were not labeled with iNOS (Figure 2C), but a few GFAP-positive astrocytes expressed TNF-α (Figure 2D, yellow cells). There may be some other cell types that release TNF-α (Figure 2D).

LPS Activates BV-2 Microglia

Twenty-four hours after LPS stimulation, the concentration of TNF-α in LPS-activated BV2 cell supernatant was 3.88 ng/mL, and that in non–LPS-activated BV2 cell supernatant was 0.20 ng/mL, detected by the DuoSet mouse TNF-α ELISA kit. Western blot showed that almost no iNOS was expressed in the BV-2 cells without LPS stimulation, but obvious expression of iNOS was induced 24 h after LPS stimulation (Figure 3, inset). Similarly, intense green fluorescence was observed in BV-2 microglia 24 h after LPS stimulation (Figure 3).

Alteration in Viability of Lung Cancer Cells Exposed to Microglial Factors

MTT assays were used to determine the viability of metastatic lung cancer cells treated with 10%, 25%, 50%, 75%, and 100% LPS-BVCM in serum-free RPMI 1640 for 12, 24, 36, and 48 h. No significant changes in viability were observed when the cancer cells were treated using BV-2 cell supernatant without LPS or with 1 μg/mL LPS added directly into serum-free RPMI 1640 at any of the above time intervals (data not shown), ruling out the possibility of a direct effect of LPS on the viability of lung cancer cells in vitro.

In general, the cytotoxicity of microglial factors to the cancer cells was time and dose dependent (Figure 4), i.e., the higher the concentration of the microglial supernatant and the longer the supernatant was applied to cancer cells, the more cancer cells died. In particular, different concentrations of the factors in the LPS-BVCM showed divergent effects

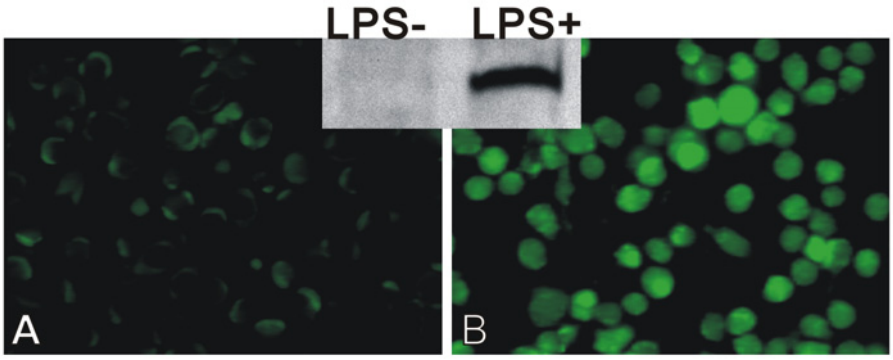

Figure 3. Upregulation of iNOS expression and NO generation in LPS-activated BV-2 microglia. Twenty-four hours after LPS stimulation, intense DAF-2DA green fluorescence can be detected in the BV-2 microglia under a fluorescent microscope (B), indicating a significant increase in NO generation, compared with slightly green color in the cells without LPS stimulation (A). In concert with the DAF-2DA reaction, iNOS protein expression detected in the Western blot is induced in the BV-2 microglia 24 h after LPS stimulation (inset). The similar β-actin bands are omitted from the picture.

on the viability of the lung cancer cells in vitro. At the same time point, a low concentration (10%) of LPS-BVCM could support survival and induce proliferation of lung cancer cells, as indicated by viability higher than 100%. Higher concentrations (50%, 75%, and 100%) of LPS-BVCM, however, exhibited stronger cytotoxicity toward the lung cancer cells. LPS-BVCM at 100% could kill 50% of cancer cells after 48-h treatment. It is worth noting that almost half of cancer cells could survive microglial cytotoxicity. Treated with the same concentration of LPS-BVCM, lung cancer cell viability showed a decrease during the initial 36 h and then no further change (25% or 75% group) or a subsequent increase (10%, 50%, or 100% group).

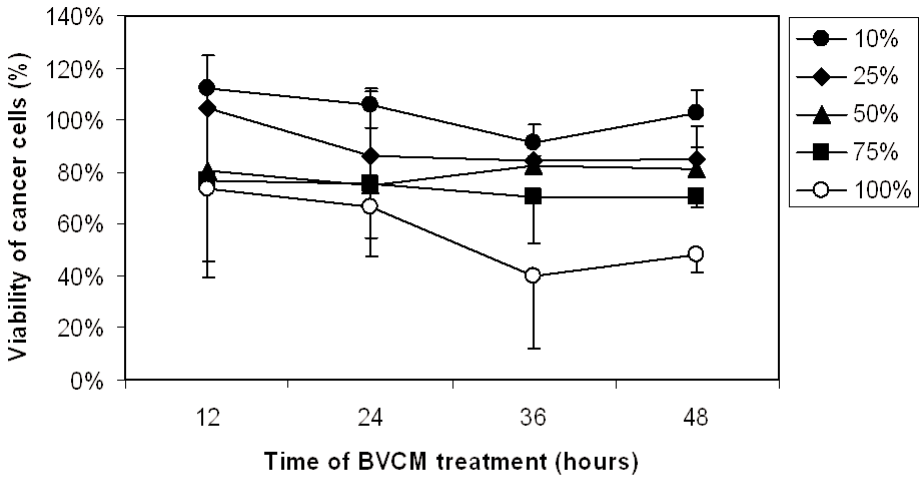

Figure 4. MTT assays of viability of lung cancer cells to detect dose- and time-dependent responses to cytotoxicity of LPS-BVCM. The LPS-BVCM was added to lung cancer cells in serum-free RPMI 1640 in concentrations of 10%, 25%, 50%, 75%, or 100%. The viability of cancer cells was determined using MTT assays at 12, 24, 36, and 48 h after the LPS-BVCM treatment. The results are presented as the mean values of 4 independent experiments and standard deviations. Significant differences ($P < 0.05$) are found between the following pairs of groups: (1) At 12 h, 10% LPS-BVCM treatment group vs. 50%, 75%, or 100% LPS-BVCM treatment group and 25% group vs. 100% group; 2) at 24 h, 10% group vs. 50%, 75%, or 100% group; 3) at 36 h, 10%, 25%, 50%, or 75% group vs. 100% group; and 4) at 48 h, 10%, 25%, or 50% group vs. 100 % group and 10% group vs. 75% group.

Cell Death Identification

Apoptosis of the lung cancer cells induced by the factors from LPS-activated BV-2 microglia was detected using BD ApoAlert Annexin V kit. The lung cancer cells showed an annexin$^-$/PI$^-$ pattern (no color) after 12-h treatment with all concentrations of LPS-BVCM. In contrast, cancer cells showed an annexin$^+$/PI$^-$ pattern (green color) after 24-, 36-, or 48-h treatment with 25%, 50%, 75%, or 100% LPS-BVCM, suggesting an early stage of apoptosis (Figure 1F). Only a few annexin$^-$/PI$^+$ cells (red color, indicating cell necrosis) and annexin$^+$/PI$^+$ (yellow color, indicating later stage of apoptotic cells) were observed. As shown in the figure 5, the percentage of lung cancer apoptotic cells induced by microglial cytotoxic factors was dose and time dependent.

Alteration in Viability of Lung Cancer Cells Exposed to TNF-α Alone

After the cancer cells were incubated with various concentrations of recombinant mouse TNF-α (corresponding to the TNF-α concentrations in 10%, 25%, 50%, 75%, and 100% LPS-BVCM), the viability of lung cancer cells was measured at 12, 24, 36, and 48 h (Figure 6). Although TNF-α did not significantly affect lung cancer cell viability in general, a trend was observed that TNF-α alone might support survival or induce proliferation of the cancer cells at higher TNF-α concentrations after longer treatment.

DISCUSSION

The current study has provided evidence that both Iba-1–positive microglia and GFAP-positive astrocytes are activated in the vicinity of metastatic lung cancer cells in the brain. An important observation was that a prominent dense "wall" of activated microglia clearly demarcated the boundary between the tumor mass and adjacent brain tissue.

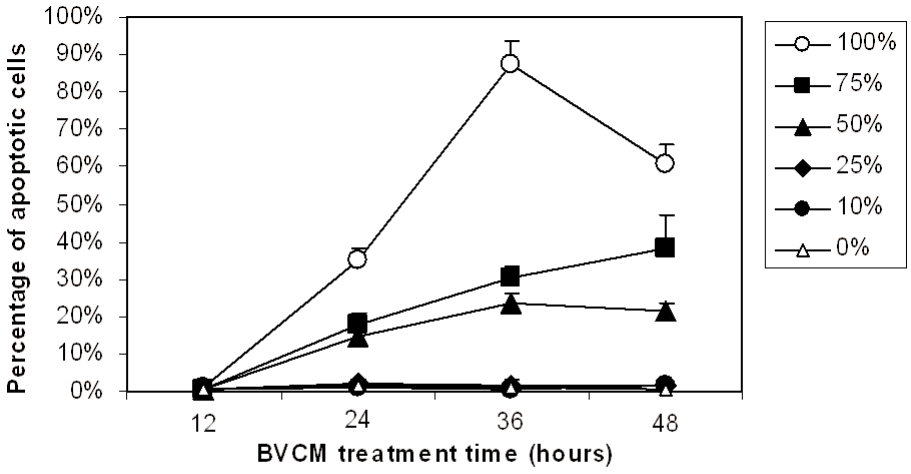

Figure 5. The percentage of annexin$^+$/PI$^-$ cells in each treatment obtained by manual counting from micrographs taken under a confocal fluorescent microscope. In 24- and 36-h treatment groups, an increasing number of apoptotic cells parallels the increasing concentration of the LPS-BVCM, indicating that microglia-induced lung cancer cell apoptosis is initially dose and time dependent. The data are presented as means and standard deviations. Statistically significant differences ($P < 0.05$) are found between the following pairs of groups: 1) At 12 h, no difference between various groups; 2) at 24 h, 0%, 10%, 25%, 50%, or 75% group vs. 100% group and 0%, 10%, or 25% group vs. 75% group; 3) at 36 h, 0%, 10%, 25%, 50%, or 75% group vs. 100% group; 0%, 10%, or 25% group vs. 75% group; and 0%, 10%, or 25% vs. 50% group; 4) at 48 h, 0%, 10%, 25%, 50%, or 75% group vs. 100% group; 0%, 10%, 25% or 50% group vs. 75% group; and 0%, 10%, or 25% vs. 50% group.

However, no such sharp boundary could be found between metastatic cancer cells and GFAP-positive astrocytes or NFH-positive neurons, indicating that microglia are possiblty the main cells directly involved with metastatic lung cancer cells. The microglial accumulation in the wall was most likely a result of microglial proliferation and/or migration, as proliferation and migration are two features of microglial activation. If the wall were formed by compression of brain parenchyma as a result of space occupation by the tumor mass, one would expect to see a similar dense GFAP-positive astrocytic or NFH-positive neuronal boundary surrounding the tumor mass, which was not the case. The highly selective cell type in the wall implies that it is actively formed by microglia. Another sign of microglial activation is morphological transformation from ramified to ameboid microglia. Indeed, the ameboid microglia, which are round in shape, could be observed in the microglial wall, and ramified microglia were in the brain region away from the tumor-brain interface. It is therefore clear that microglia have the propensity to become activated in the brain region with metastasis of lung cancer cells.

What then is the source of the signals that activate microglia? It is clear that degenerating neurons can activate microglia, although the nature of the signal has yet to be identified. It is not certain, however, if the growth of cancer cells and thereafter space occupation by the tumor mass could directly lead to any neuronal degeneration or even neuronal death. iNOS, a protein mediating the synthesis of NO, is found in brain microglia and peripheral macrophages (24) and in astrocytes (25,26). Normally, activated microglia show a significant increase in the expression level of iNOS (27). The excessive amount of NO could result in neuronal degeneration in vitro (28); upregulation of iNOS has been reported to augment neurodegeneration in an animal model of Parkinson disease (29). In the current study, iNOS-positive cells scattered in the brain tissue in the vicinity of the tumor mass have yet to be identified, as they were shown to be neither lectin-positive microglia nor GFAP-positive astrocytes. However, a strong expression of iNOS in metastatic lung cancer cells has been revealed by the intense staining of anti-iNOS antibody, suggesting that much NO might be generated in the cancer cells and implying the possible role of NO in the survival of these metastatic cancer cells. Although NO may potentiate cancer cell survival in the local environment (30), neurons next to these cancer cells might be affected by NO released from cancer cells. The neurons affected by NO might therefore release signals to activate microglia, resulting in the formation of the microglial wall in the surgical biopsy tissues. However, based on our current results, we cannot rule out the possibility that cancer cells could activate microglia directly. In fact, a recent paper has shown that NO could upregulate the expression of complement receptor type 3 α-subunit (CD-11b) in the microglia (31), providing the possibility for cancer cells directly activating microglia.

Our next question is, what is the functional significance of activated microglia in the brain region with metastatic cancer cells? The surgically removed brain tissues in this study represented only the late stage of the disease, in which the metastatic lung cancer cells have already successfully homed and consolidated in the brain parenchyma, indicating the failure of the cytotoxic defense mechanism against malignant cells in the brain. As the key immune cells in the CNS (32), activated microglia are expected to provide such cytotoxic defense, but it appears that they could not stop the development of the metastatic lung cancer cells in the patients examined. The reason for this failure might be explained from following two aspects: dual functions of microglia and resistance of metastatic cancer cells against the brain's immune defense.

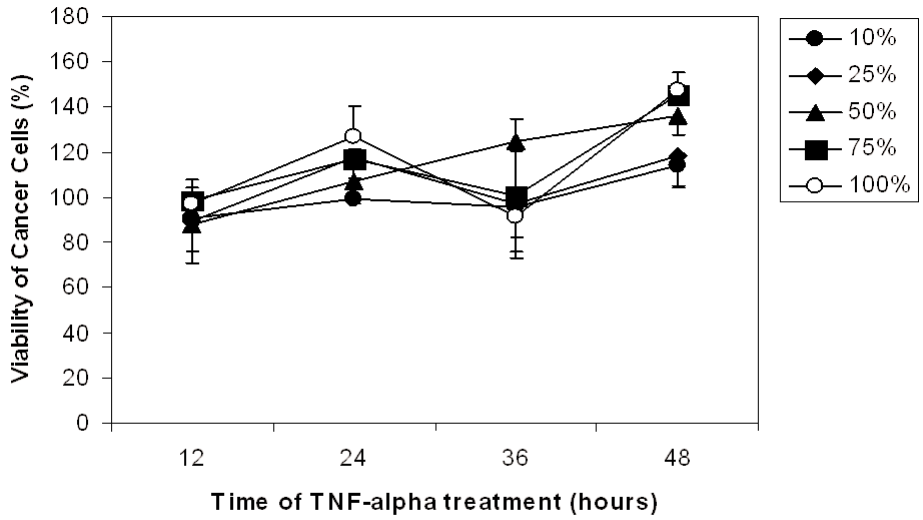

Figure 6. MTT assays of the cellular effect of TNF-α on viability of the lung cancer cells. Recombinant mouse TNF-α at 0.388, 0.97, 1.94, 2.91, and 3.88 ng/mL was cocultured with the lung cancer cells for 12, 24, 36, and 48 h. The viability of the lung cancer cells was determined using MTT assays. No significant decrease in viability can be noted, while increases in viability can be observed in at 24 and 48 h after treatment with higher concentrations of TNF-α. The data are presented as means and standard deviations. Statistically significant differences ($P < 0.05$) are found between the following pairs of groups: 1) At 24 h, 0.338 ng/mL, equal to 10% LPS-BVCM treatment group vs. 3.88 ng/mL, 100% LPS-BVCM treatment group; 2) At 48 h, 0.338 ng/mL, 10% group vs. 2.91 ng/mL, 75% or 3.88 ng/mL,

The first possibility is that the microglial reaction induced by metastatic cancer cells could be protective/trophic responses. Cytotoxicity of microglia has been studied for a long time in neurodegenerative diseases and CNS injury. Similar to previous studies showing that LPS-stimulated microglia have pancytotoxicity to a neuronal cell line (20) and primary cultured neurons (33), we show here that LPS-induced microglial cytotoxicity to metastatic lung cancer cells is concentration and time dependent. Within the current experimental time frame (up to 48 h), the results from both viability tests and annexin-V staining have revealed that more cancer cells could be killed via apoptosis the higher the concentrations of factors released from LPS-activated microglia and the longer the treatment was applied to the cancer cells. However, the dual functions of activated microglia were unexpectedly associated with the concentration of the LPS-activated microglial supernatant applied. At a lower concentration of supernatant (10%), the metastatic lung cancer cells exhibited an increase in viability. The viability gradually decreased and more apoptotic cells were induced as the concentration of LPS-stimulated microglial supernatant increased. In consideration that LPS stimulation may also result in the release of growth factors and some cytokines that could potentially elaborate the immune response (34), the balance between microglial protective/trophic function and cytotoxic/destructive function might be directly adjusted by the relative amounts of various factors released from activated microglia. At a certain stage of interaction between microglia and metastatic cancer cells, microglia might produce fewer cytotoxic factors and more protective factors, providing a favorable niche for the cancer cells.

Based on our in vivo observation, the microglia have exhibited both signs of activation (increase in number in the wall, transformation from resting to ameboid) and inactivation (no iNOS or TNF-α expression), indicating that metastatic cancer cells may modulate microglial functions. TNF-α is a cytokine released by immune cells, including activated microglia. While it can cause cytolysis of certain tumor cell lines, TNF-α can stimulate cell proliferation and induce cell differentiation under certain conditions (35). In the CNS, TNF-α released from reactive microglia (36) or astrocytes (37) could promote neurodegeneration. However, in the brain sections examined, TNF-α–positive cells (only some of them were astrocytes) were found scattered in the brain region near the tumor masses, although there was a dense wall of Iba-1–positive microglia, suggesting that most of Iba-1–positive microglia in the microglial wall could not release TNF-α and the opportunity for TNF-α to destroy the metastatic lung cancer cells would be slim. Similarly, in astrocytic tumors, the expression of TNF-α was not observed in peritumoral brain tissue (38). In our in vitro study, pure TNF-α at the same amount detected from the LPS-activated microglial supernatant failed to eradicate the metastatic lung cancer cells, suggesting that TNF-α requires other synergistic microglial factors to kill tumor cells. Our previous observation, that almost all LPS-activated microglia produced NO in vitro (20), and our current in vivo observation, that most activated Iba-1– or lectin-positive microglia could not express iNOS, suggest that microglial activation could be stimulus specific, i.e., the factors released from tumor-activated microglia could be different from factors released from LPS-activated microglia. Microglia response to different stimuli may lead to variation in factors released from activated microglia and therefore shift their dual functions from destruction/cytotoxicity to protection and vice versa. The Iba-1- or lectin-positive cells in the vicinity of the tumor mass did not express iNOS and TNF-α, representing some features of polarized M2 macrophages which are differentiated from recruited monocytes (39). The M2 macrophages may have the capacity to promote proliferation of the tumor cells

but not cytotoxicity to kill tumor cells (40). The question on whether metastatic lung cancer cells could selectively attract 1 type of monocytes from the peripheral monocyte pool should be addressed in the future.

Some metastatic cancer cells survived the microglial reactions in vitro. After application of LPS-BVCM treatment for 48 h, the viability of the cancer cells showed more or less an increase compared with that at 36 h. Two reasons may contribute to this observation. First, the effective components in the activated BV-2 supernatant, such as TNF-α, may be degraded by 48 h. Second, not all cancer cells are sensitive to microglial cytotoxicity, and some cancer cells may have become resistant. Therefore, after 36-h treatment, the cytotoxic-resistant/insensitive tumor cells may survive the microglial toxic attack and proliferate in later stage of the assays. Although the mechanism involved in such resistance/insensitivity (which might be due to genetic variance) is still unclear, the metastatic lung cancer cells in the brain have demonstrated their ability to preclude the penetration of the Iba-1–positive microglia into the central region of the tumor mass, leaving behind an accumulation of a wall of microglia and providing a higher chance for cancer cell growth without external interference from the brain immune cells, such as microglia. In concert with this view, Strik et al. (41) have reported that overall a small numbers of $CD68^+$ monocytes/microglia (possibly including monocytes in capillaries) were observed in 67 pooled primary and metastatic or malignant (4.92% ± 1.48% in 9 cases of brain metastatic adenocarcinoma) and benign brain tumors, compared with microglial accumulation in the pathological foci of other CNS injury and diseases. In contrast to the current study, however, Strik et al. have also found considerable $CD68^+$ cell infiltration (12.68% and 14.51%) in 2 of 9 cases of brain metastatic adenocarcinoma. The possible reason for the variation in the counting of $CD68^+$ monocytes/microglia could be due to variation in distribution of capillaries in tumor parenchyma or stage of metastatic tumor development.

In conclusion, on one hand, microglial accumulation as a result of migration and proliferation and an ameboid appearance of microglia have pointed out that microglia could actively respond to the metastatic lung cancer cells in the brain and tightly "encapsulate" the tumor mass. On the other hand, the lack of positivity to either iNOS or TNF-α in the double-labeling experiments indicates that microglial immunological functions—i.e., possibly cytotoxic activity, phagocytosis, and antigen presentation—are inactivated in the tumors investigated. Although LPS-activated microglia can kill some metastatic cancer cells in vitro, the mechanism involved in activation of microglia in the brain sections is obviously different from that of LPS stimulation. It is therefore of importance to elucidate how metastatic lung cancer cells could modulate microglial functions and what factors microglia might release in response to brain metastatic lung cancer cells, especially at an earlier metastatic stage.

ACKNOWLEDGMENT

This work was supported by the grant (NMRC/1037/2006) from National Medical Research Council, Singapore.

REFERENCES

1. Jafri NF, Ma PC, Maulik G, Salgia R. (2003) Mechanisms of metastasis as related to receptor tyrosine kinases in small-cell lung cancer. *J. Environ. Pathol. Toxicol. Oncol.* 22:147-65.
2. Schuette W. (2004) Treatment of brain metastases from lung cancer: chemotherapy. *Lung Cancer* 45:S253-7.
3. Zabel A, Debus J. (2004) Treatment of brain metastases from non-small-cell lung cancer (NSCLC): radiotherapy. *Lung Cancer* 45:S247-52.
4. Pottgen C, Stuschke M. (2001) The role of prophylactic cranial irradiation in the treatment of lung cancer. *Lung Cancer* 33:S153-8.
5. Nakamura Y. (2002) Regulating factors for microglial activation. *Biol. Pharm. Bul.* 25:945-53.
6. Kas HS. (2004) Drug delivery to brain by microparticulate systems. *Adv. Exp. Med. Biol.* 553: 221-30.
7. Longley DB, Johnston PG. (2005) Molecular mechanisms of drug resistance. *J. Pathol.* 205:275-92.
8. Kreutzberg GW. (1996) Microglia: a sensor for pathological events in the CNS. *Trends Neurosci.* 19:312-8.
9. Chen JW et al. (2005) Tumor-associated macrophages: the double-edged sword in cancer progression. *J. Clin. Oncol.* 23:953-64.
10. Morimura T, Neuchrist C, Kitz K, Budka H, Scheiner O, Kraft D, Lassmann H. (1990) Monocyte subpopulations in human gliomas: expression of Fc and complement receptors and correlation with tumor proliferation. *Acta Neuropathol. (Berl)* 80:287-94.
11. Roggendorf W, Strupp S, Paulus W. (1996) Distribution and characterization of microglia/macrophages in human brain tumours. *Acta Neuropathol. (Berl)* 92:288-93.
12. Badie B, Schartner J. (2001) Role of microglia in glioma biology. *Microsc. Res. Tech.* 54:106-13.
13. Huettner C, Czub S, Kerkau S, Roggendorf W, Tonn JC. (1997) Interleukin 10 is expressed in human gliomas in vivo and increases glioma cell proliferation and motility in vitro. *Anticancer Res.* 17:3217-24.
14. Platten M et al. (2003) Monocyte chemoattractant protein-1 increases microglial infiltration and aggressiveness of gliomas. *Ann. Neurol.* 54:388-92.
15. Taniguchi Y, Ono K, Yoshida S, Tanaka R. (2000) Antigen-presenting capability of glial cells under glioma-harboring conditions and the effect of glioma-derived factors on antigen presentation. *J Neuroimmunol.* 111:177-85.
16. Wagner S, Czub S, Greif M, Vince GH, Suss N, Kerkau S, Rieckmann P, Roggendorf W, Roosen K, Tonn JC. (1999) Microglial/macrophage expression of interleukin 10 in human glioblastomas. *Int. J. Cancer* 82:12-6.
17. Bettinger I, Thanos S, Paulus W. (2002) Microglia promote glioma migration. *Acta Neuropathol. (Berl)* 103:351-5.
18. Hao C et al. (2002) Cytokine and cytokine receptor mRNA expression in human glioblastomas: evidence of Th1, Th2 and Th3 cytokine dysregulation. *Acta Neuropathol. (Berl).* 103:171-8.
19. Choucair AK et al. (1986) Development of multiple lesions during radiation therapy and chemotherapy in patients with gliomas. *J. Neurosurg.* 65: 654-58.
20. Ito D, Imai Y, Ohsawa K, Nakajima K, Fukuuchi Y, Kohsaka S. (1998) Microglia-specific localisation of a novel calcium binding protein, Iba1. *Mol. Brain Res.* 57:1-9.
21. Blasi E, Barluzzi R, Bocchini V, Mazzolla R, Bistoni F. (1990) Immortalization of murine microglial cells by a v-raf/v-myc carrying retrovirus. *J. Neuroimmunol.* 27:229-37.
22. He BP, Wen W, Strong MJ. (2002) Activated microglia (BV-2) facilitation of TNF-alpha-mediated motor neuron death in vitro. *J. Neuroimmunol.* 128:31-8.
23. Kojima H, Nakatsubo N, Kikuchi K, Urano Y, Higuchi T, Tanaka J, Kudo Y, Nagano T. (1998) Direct evidence of NO production in rat hip-

pocampus and cortex using a new fluorescent indicator: DAF-2 DA. *Neuroreport* 9:3345-8.
24. Gebicke-Haerter PJ. (2001) Microglia in neurodegeneration: molecular aspects. *Microsc. Res. Tech.* 54:47-8.
25. Jana M, Anderson JA, Saha RN, Liu X, Pahan K. (2005) Regulation of inducible nitric oxide synthase in proinflammatory cytokine-stimulated human primary astrocytes. *Free Radic. Biol. Med.* 38:655-64.
26. Kozuka N, Itofusa R, Kudo Y, Morita M. (2005) Lipopolysaccharide and proinflammatory cytokines require different astrocyte states to induce nitric oxide production. *J. Neurosci. Res.* 82:717-28.
27. Lechner M, Lirk P, Rieder J. (2005) Inducible nitric oxide synthase (iNOS) in tumor biology: the two sides of the same coin. *Semin. Cancer Biol.* 15:277-89.
28. Bossy-Wetzel E, Talantova MV, Lee WD, et al. (2004) Crosstalk between nitric oxide and zinc pathways to neuronal cell death involving mitochondrial dysfunction and p38-activated K+ channels. *Neuron* 41:351-365.
29. Liberatore GT, Jackson-Lewis V, Vukosavic S, et al. (1999) Inducible nitric oxide synthase stimulates dopaminergic neurodegeneration in the MPTP model of Parkinson disease. *Nat. Med.* 5:1403-1409.
30. Land SC, Rae C. (2005) iNOS initiates and sustains metabolic arrest in hypoxic lung adenocarcinoma cells: mechanism of cell survival in solid tumor core. *Am. J. Physiol. Cell Physiol.* 289:C918-933.
31. Roy A, Fung YK, Liu X, Pahan K. (2006) Up-regulation of microglial cd11b expression by nitric oxide. *J. B. C.* (In press)
32. Gonzalez-Scaranol F, Baltuch G (1999) Microglia as mediators of inflammatory and degenerative diseases. *Annu. Rev. Neurosci.* 22:219-240.
33. Le W, Rowe D, Xie W, Ortiz I, He Y, Appel SH. (2001) Microglial activation and dopaminergic cell injury: an in vitro model relevant to Parkinson's disease. *J. Neurosci.* 21:8447-8455.
34. Elkabes S, DiCicco-Bloom EM, Black IB. (1996) Brain microglia/macrophages express neurotrophins that selectively regulate microglial proliferation and function. *J. Neurosci.* 16: 2508-2521.
35. Vadlamani L, Iyengar S (2004) Tumor Necrosis Factor α Polymorphism in Heart Failure/ Cardiomyopathy. *Congest Heart Fail.* 10:289-292.
36. Schubert P, Ogata T, Miyazaki H, Marchini C, Ferroni S, Rudolphi K. (1998) Pathological immuno-reactions of glial cells in Alzheimer's disease and possible sites of interference. *J. Neural Transm. Suppl.* 54:167-174.
37. Wu YP, Mizukami H, Matsuda J, Saito Y, Proia RL, Suzuki K. (2005) Apoptosis accompanied by up-regulation of TNF-alpha death pathway genes in the brain of Niemann-Pick type C disease. *Mol. Genet. Metab.* 84:9-17.
38. Roessler K, Suchanek G, Breitschopf H, Kitz K, Matula C, Lassmann H, Koos WT. (1995) Detection of tumor necrosis factor-alpha protein and messenger RNA in human glial brain tumours: comparison of immunohistochemistry with in situ hybridization using molecular probes. *J. Neurosurg.* 83:291-297.
39. Mantovani A, Sozzani S, Locati M, Allavena P, Sica A. (2002) Macrophage polarization: tumor-associated macrophages as a paradigm for polarized M2 mononuclear phagocytes. *Trends Immunol.* 23:549-555.
40. Dinapoli MR, Calderon CL, Lopez DM. (1996) The altered tumoricidal capacity of macrophages isolated from tumor-bearing mice is related to reduce expression of the inducible nitric oxide synthase gene. *J. Exp. Med.* 183:1323-1329.
41. Strik HM, Stoll M, Meyermann R. (2004) Immune cell infiltration of intrinsic and metastatic intracranial tumours. *Anticancer Res.* 24:37-42.